Theor Chem Account (2007) 118:947–957
DOI 10.1007/s00214-007-0378-3

REGULAR ARTICLE

Study of hydrogen-bonded clusters of 2-methoxyphenol–water

Seifollah Jalili · Mojdeh Akhavan

Received: 28 May 2007 / Accepted: 9 July 2007 / Published online: 27 July 2007

Abstract Various hydrogen-bonded clusters of 2-methoxyphenol (2MP) with water have been analyzed using ab initio methods and Atoms in Molecules (AIM) theory. The intramolecular hydrogen bond energy (and enthalpy) for 2MP was evaluated from two different methods. The results of rotational barriers method are in better agreement with experimental data. Binding energies, vibrational frequencies and geometrical parameters were examined and compared for these complexes. It was shown that in the most stable complex, water acts both as a donor and an acceptor. The "bifurcated" complex was shown to be relatively stable based on energy values. Atoms in Molecules and Natural Bond Orbital (NBO) analysis were used to confirm the existence of hydrogen bonds and to compare the strengths of them. The results obtained from quantum mechanical, AIM and NBO calculations are in agreement with each other.

Keywords 2-Methoxy phenol (2MP) · Antioxidant · Bond dissociation enthalpy (BDE) · Microhydration · Bifurcated hydrogen bond · Atoms in molecules (AIM) theory

1 Introduction

Many natural antioxidants important in the protection of human low-density lipoproteins, such as α-tocopherol (vitamin E) and ubiquinol-10 ($Q_{10}H_2$) are alkoxy-substituted phenolic compounds [1]. These compounds can trap chain-carrying peroxyl radicals by donating a hydrogen atom. In addition, phenolic compounds are widely used as additives in food technology to reduce the rate of oxidative degradation. The antioxidant activity of substituted phenols is a consequence of the relatively low phenolic O–H bond dissociation enthalpy [BDE (O–H)].

Various experimental and theoretical techniques [1–3] have been applied to the measurement of phenolic O–H BDE's. DFT calculations on phenol and a large number of its derivatives with methyl, methoxyl and amino substituents have yielded BDE's in good agreement with experimental results [4].

When a group with hydrogen accepting capacity is substituted in the ortho-position of phenols, it establishes an intramolecular hydrogen bond with the OH group. One of such substituents is the methoxy group, which is shown to act as a proton acceptor in different types of hydrogen bonds [5]. In ubiquinol-10 the phenolic hydrogens are intramolecularly bonded to methoxy groups. Thus, the antioxidant activity of ubiquinol-10 involves the abstraction of an intramolecularly hydrogen-bonded phenolic hydrogen.

The solvent has a dramatic effect on the rate constant for hydrogen abstraction from phenolic compounds. Hydrogen abstraction is inhibited when a solvent with hydrogen-bond accepting capacity (HBA) forms a linear intermolecular hydrogen bond with the phenolic hydrogen [2]. In contrast; phenolic hydrogens involved in an intramolecular hydrogen bond are readily abstractable. Spencer et al. [6,7], used IR spectroscopy and found that HBA solvents such as diethyl ether, THF, and di-*n*-butyl sulfide did not disrupt the intramolecular hydrogen bond in 2-methoxyphenol (2MP). Only with DMSO, a change in the concentration of intramolecularly hydrogen bonded molecule was observed.

S. Jalili (✉) · M. Akhavan
Department of Chemistry, K. N. Toosi university of Technology,
P. O. Box 15875-4416, Tehran, Iran
e-mail: sjalili@kntu.ac.ir

S. Jalili · M. Akhavan
Computational Physical Sciences Research Laboratory,
Department of Nano-Science, Institute for Studies in Theoretical Physics and Mathematics (IPM),
P.O. Box 19395-5531, Tehran, Iran

Fig. 1 Model systems

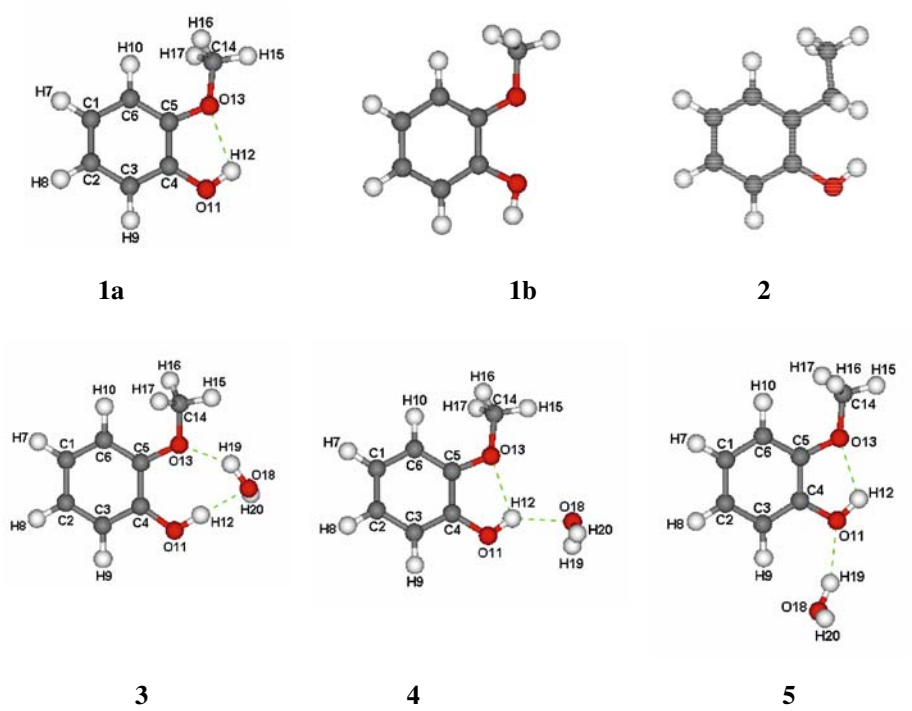

He concluded that DMSO, which is a strong electron donor, can disrupt the intramolecular hydrogen bond and subsequently form an intermolecular hydrogen bonded complex [6]. Nevertheless, kinetic studies on solvent effects suggest that an additional interaction (that is, an intermolecular hydrogen bond) can be formed between the intramolecularly bonded hydrogen and a solvent molecule [1] and it is believed that the abstraction of such doubly hydrogen bonded phenolic hydrogen atoms does not occur. This type of three-centered or "bifurcated" hydrogen bond involves one donor and two acceptors. The H atom is surrounded by three electronegative atoms, having one covalent and two hydrogen bonds with them.

Bifurcated hydrogen bonds play important roles in many chemical and biological systems, e.g., proteins [8], nucleotides [9] and carbohydrates [10]. Bifurcated hydrogen bonds are also present in many simple molecular complexes [11–13], and gas-phase molecules [14]. Spectroscopic studies confirm the existence of bifurcated hydrogen bonds in solutions containing substituted phenols with different acceptor groups [15]. It is also found, using spectroscopic and computational methods, that when 2MP is dissolved in toluene, a bifurcated hydrogen bond is formed, in which the π-electrons of aromatic ring act as an acceptor for hydrogen bond [16].

Despite the studies that suggest a bifurcated interaction, in which the intramolecular hydrogen bond of 2MP is retained [1,3,16], Brutschy and Wu showed in a study of 2-methoxyphenol/water clusters that in the 1:1 complex the intramolecular hydrogen bond between OCH_3 and OH groups is destroyed and the water molecule inserts between these groups and forms a cyclic structure [17]. Their results were in agreement with experimental IR spectra of complexes. However, they have not taken into account the possibility of a bifurcated hydrogen bond. There are also a number of experimental and computational works on other microsolvated structures. Mikami [18] studied the hydrogen-bonded clusters of methyl salicylate with H_2O, CH_3OH, and NH_3 using infrared spectroscopy. He concluded that the intramolecular hydrogen bond in methyl salicylate is retained in these clusters. Other examples of microsolvated structures involve 1:1 clusters of 2-aminopyridine with ammonia [19], hydrogen bonded clusters of 2-fluoropyridine with water [20], 2-naphtol– $(NH_3)_n$ hydrogen bonded clusters [21], 7-azaindole clusters [22], and other systems [23–26]. These studies are important to give insights into solute–solvent interactions.

The aim of this study is to compare the structure, energetics and vibrational frequencies of various 1:1 clusters of 2-methoxyphenol–water, taking into account the possibility of a bifurcated hydrogen bond. When a methoxy group is substituted in the ortho-position of phenol, an intramolecular hydrogen bond is formed between two groups. The energy of this hydrogen bond (E_{HB}) can be evaluated as the energy difference between the *chelate* (hydrogen-bonded) conformation (**1a** in Fig. 1) and the conformation having the O–H (donor) group outside rotated by 180° (*open*, or non-hydrogen-bonded conformation, **1b**) [27]. Another method is the comparison of rotational barriers (RBs) calculated in the presence and in the absence of hydrogen bond [28]. The

E_{HB} is determined by comparing the O–H RBs found in 2MP molecule and the corresponding one evaluated in a hydrogen bond free reference compound. This compound is obtained by substituting the methoxy group with an ethyl group (**2** in Fig. 1). The results of these two methods are compared to other experimental and theoretical data. In the second step, three different complexes with H_2O (**3**, **4**, **5** in Fig. 1) have been optimized and binding energies [including corrections for zero-point energy and basis set superposition error, BSSE], vibrational frequencies, and structural parameters of them calculated and compared. In order to complete our qualitative and quantitative studies on these clusters, we have performed "atoms in molecules" (AIM) analysis of electron density. In addition, Natural Bond Orbital (NBO) analysis was used to understand the hydrogen-bonded systems in terms of the various donor–acceptor interactions. These calculations enable us to confirm the existence of hydrogen bonds based on a number of criteria [29] and to compare the strength of various hydrogen bonds.

1.1 The theory of atoms in molecules

Bader's "Atoms in Molecules" theory [30,31] is a valuable tool in the investigation of cyclic [27,32] and bifurcated [29,32,34] hydrogen bonds and proton transfer reactions [35]. Using this theory we can characterize hydrogen bonds solely from the (total) electron density, ρ. The key concept in AIM theory is the gradient vector field of electron density; $\nabla\rho$. Successive infinitesimal gradient vectors form a gradient path, which is perpendicular to electronic isodensity surface at every point. These paths come from infinity and reach to special points called *attractors*. All nuclei are attractors and the collection of all gradient paths terminating to each nucleus is called an *atomic basin*. These basins are separated by interatomic surfaces and define an *atom* in the molecule. Atomic properties are calculated by integrating over these atomic basins.

It is also possible to define a bond within the context of AIM theory. Some gradient paths arriving at a nucleus do not come from infinity but from a point in between two nuclei, called a bond critical point (BCP). Critical points are exterma in the electron density or points in space where the gradient of $\rho(r)$ vanishes. These BCPs link two nuclei through a special gradient path, called the *bond path*. A BCP is a minimum along the bond path and a maximum along the interatomic surface, perpendicular to the bond path. There is also a ring critical point (RCP), which may be characterized by a minimum value of ρ in the plane of ring, and a maximum with respect to the multifold axis of rotation.

The Hessian of $\rho(r)$ is a 3×3 matrix of second derivatives which diagonalizes to yield three eigenvalues λ_1, λ_2 and λ_3. The sum $\lambda_1+\lambda_2+\lambda_3=\nabla^2\rho(r)$ is the Laplacian of electron density and $\varepsilon=(\lambda_1/\lambda_2)-1$ is the ellipticity. The ellipticity describes the symmetry of the electron density distribution along the bond path. It is found that closed-shell interactions such as ionic bonds, hydrogen bonds and van der Waals' interactions should have a positive $\nabla^2\rho$ and a relatively small value of ρ.

Eight concerted effects within the AIM formalism have been considered as the suitable criteria for hydrogen bonding [29]. The first three of them are: (1) the existence of a bond path, containing a BCP between the donor hydrogen atom and the acceptor, (2) the value of density $\rho(r)$ at the BCP and (3) the value of the Laplacian of the density at the BCP. These three criteria together with ellipticity and distance to a RCP will be referred to as "BCP" criteria [34].

2 Computational details

Ab initio calculations were carried out with the GAUSSIAN 03 program [36] and AIM analysis was performed using AIM 2000 code [37] implemented on a Pentium IV computer. Geometry optimizations and frequency calculations were performed using the B3LYP functional and MP2 method, with the 6-31G(d,p) basis set. The frequencies from these methods have been shown to be in good agreement with experimental data [38]. The zero point vibrational energy (ZPE) values obtained from B3LYP and MP2 methods were scaled by 0.9806 and 0.9608 factors [3,39], respectively. Single point energy calculations were performed using B3LYP/6-31+G(d,p) and MP2/6-31+G(d,p) levels of theory in order to take into account the effects of diffuse functions that are important for hydrogen bond energies [40].

The RBs for chelate (**1a**) and reference (**2**) molecules were evaluated by scanning the potential energy surface with an increment size of 5° (for each step the molecular geometry was optimized) toward the maximum energy point. The maximum and minimum energy structures were optimized, followed by frequency and single point calculations to compute RBs and E_{HB}. The intramolecular BSSE corrections were calculated by Jensen's approach [41].

Several trial structures of 2MP:H_2O complexes were examined to find the stable isomers that are depicted in Fig. 1 (**3**, **4**, **5**). Calculated structures were optimized at B3LYP/6-31G(d,p) and MP2/6-31G(d,p) levels of theory. The bifurcated complex (**4**) had to be optimized by using geometrical constraints necessary to maintain its geometry, because such systems are located on saddle points of the potential energy surface [11]. The calculated vibrational frequencies were scaled by suitable scale factors to minimize the difference with experimental data. For calculating the binding energies, BSSE corrections were estimated using the counterpoise (CP) method. According to this method, the interaction energy in

a complex (AB) is calculated from the following relations:

$$E_{\text{int,cp}} = E(\text{AB}, r_c)^{\text{AB}} - E(\text{A}, r_c)^{\text{AB}} - E(\text{B}, r_c)^{\text{AB}} + E_{\text{def}}$$
$$E_{\text{def}} = [E(\text{A}, r_c) - E(\text{A}, r_e)] + [E(\text{B}, r_c) - E(\text{B}, r_e)]$$

The label r_c is used to indicate the geometry of complex (AB) and r_e indicates the geometry of separate reactants (A and B). The superscript AB denotes a calculation with the full basis set of complex. E_{def} is the energy required for the deformation of components A and B from their equilibrium geometries to the complex geometries.

Wavefunction analysis was done by using NBO method [42,43], including Natural Population Analysis (NPA) [44]. These calculations were performed with NBO 3.0 program [45] implemented in Gaussian 03.

3 Results and discussion

3.1 Energies

Intramolecular hydrogen bond energy calculated from two different methods, namely chelate-open energy difference and RBs, are given in Table 1. The results obtained from the difference in RBs are lower than the other method. The (absolute value of) MP2 hydrogen bond energies are higher than the DFT results. It seems that unlike the ZPE correction that lowers the HB energy in both methods, the BSSE correction increases the energy in the first method, but not in the second one. The RBs' results are therefore more reasonable. The hydrogen bond enthalpy of 2MP is also calculated from two methods. The experimental enthalpy is −4.3 kcal/mol [3]. The enthalpy obtained from RBs with MP2 method is in excellent agreement with this experimental value.

Three hydrogen-bonded complexes of 2MP phenol and water, as shown in Fig. 1 were considered in this work. In **3**, water acts as a hydrogen bond acceptor for hydroxy group and a hydrogen bond donor for methoxy group. Water inserts between two groups and the intramolecular hydrogen bond is lost. In **4**, water molecule acts as a second hydrogen bond acceptor for phenolic hydrogen and a so-called "bifurcated" hydrogen bond is formed in which the phenolic hydrogen is surrounded by three oxygen atoms from water and hydroxy and methoxy groups. In the last structure, **5**, water donates one hydrogen atom to phenolic oxygen atom, while the intramolecular hydrogen bond is preserved. Table 2 shows the energy values for 2-methoxy phenol and three hydrogen-bonded complexes. Structure **3** is the global energy minimum (taking into account the scaled zero point energy corrections). The energies of **4** and **5** relative to this compound from DFT calculations are 0.213 and 0.552 kcal/mol, respectively, while the corresponding MP2 values are 0.998 and 1.155 kcal/mol. It seems that the structure with bifurcated hydrogen bond (**4**) is slightly more stable than the structure with separate inter- and intramolecular hydrogen bonds (**5**).

The situation is different with binding energies (Table 3). Without including any corrections, the binding energy of **3** is the most and structure **4** has the lowest binding energy. Again the MP2 values are larger than their DFT counterparts. However, including the ZPE correction considerably decreases the binding energy and the trend changes. Now compound **4** has a larger binding energy than **5**, in accord with energy data (Table 2). Considering the BSSE correction has not a uniform effect. The data obtained after this correction are very similar to each other.

Table 1 Intramolecular hydrogen bond energy (kcal/mol) for 2MP (6-31+G** energies on 6-31G** geometries)

Energy	Method 1[a]		Method 2[b]	
	B3LYP	MP2	B3LYP	MP2
E_{HB}	−4.62	−4.92	−4.15	−4.53
E_{HB} including ZPE	−4.44	−4.69	−3.95	−4.43
E_{HB} including ZPE and BSSE	−5.09	−5.37	−3.83	−4.25
HB enthalpy	−5.11	−6.33	−3.91	−4.29

[a] Calculated from energy difference between chelate and open conformations

[b] Calculated from difference in rotational barriers between 2MP and a reference

3.2 Vibrational frequencies

Table 4 shows important calculated vibrational frequencies for 2MP and its complexes. The bifurcated structure shows one imaginary frequency consistent with a saddle point on the potential energy surface. DFT and MP2 Results obey a similar trend in all compounds, but the MP2 values are smaller than the corresponding DFT ones. DFT includes electron correlation at lower computational cost, but the MP2 frequencies are closer to experimental values (for example, for phenol [17]). Therefore, the following discussion is based on MP2 results. Similar conclusions can be drawn from DFT results.

As it is clear from Table 4, the calculated stretching vibrational frequency for hydroxy group in 2MP (**1a**) is 3, 585.2 cm^{-1}. It shows a red shift of about 50 cm^{-1} relative to phenol's O–H stretching frequency (3, 634.1 cm^{-1}). This red shift reflects an intramolecular hydrogen bond in which the hydroxy group of 2MP acts as a donor.

The O–H frequency in structures **3**, **4** and **5** is 3,423.1, 3,463.7 and 3, 575.4 cm^{-1}, respectively. In **3**, O–H acts as a donor in an intermolecular hydrogen bond with water molecule. This hydrogen bond is stronger than the original intramolecular hydrogen bond in 2MP. Therefore, the O–H frequency is red-shifted by 162.1 cm^{-1} relative to **1a**.

Table 2 Energy values for 2-methoxy phenol (2MP) and three complexes

System	Energy (au)		Scaled ZPE (au)		Dipole moment (D)	
	B3LYP	MP2	B3LYP	MP2	B3LYP	MP2
1a	−422.02457	−420.77658	0.13510	0.13316	2.8702	3.0950
3	−498.46655	−497.02074	0.15944	0.15776	3.5722	3.9023
4	−498.46484	−497.01783	0.15807	0.15644	1.7109	1.2167
5	−498.46523	−497.01855	0.15900	0.15741	4.9646	5.1486

Table 3 Calculated binding energies (kcal/mol) for three hydrogen bonded complexes (6-31+G** energies on 6-31G** geometries)

Complex	**3**		**4**		**5**	
	B3LYP	MP2	B3LYP	MP2	B3LYP	MP2
Binding energy	5.04	6.98	3.97	5.16	4.21	5.61
Binding energy + ZPE	2.92	4.95	2.70	3.96	2.36	3.80
Binding energy + ZPE + BSSE	1.83	1.82	1.82	1.93	1.66	2.04

Similarly, the additional intermolecular hydrogen bond of phenolic O–H with water in **4** causes a 121.5 cm^{-1} reduction in the calculated frequency. However, in **5** this red shift is only 9.8 cm^{-1}. This is because the intramolecular H-bond in 2MP is preserved and the phenolic hydrogen is not involved in an additional hydrogen bond. Similar results will be deduced from structural changes. The red shift for the bifurcated structure (**4**) is in accord with the experimental value of 122 cm^{-1} [17].

Now we focus on vibrational frequencies of O–H bonds in water. The calculated vibrational frequency for bonded O–H of water in **3** is 3, 576.7 cm^{-1}. The vibrational frequency for symmetric O–H stretch in an isolated water molecule is 3, 648.0 cm^{-1}. The observed red shift in this frequency (71.3 cm^{-1}) shows that this O–H is involved in a hydrogen bond as a donor. Similar red shift is observed for structure **5**, in which the bonded O–H stretch of water is red-shifted by 42.1 cm^{-1}. For **4**, there is a little difference in O–H frequencies relative to pure water, because in this case water is only a hydrogen-bond acceptor. In general the red shift is observed when an O–H group is a hydrogen-bond donor, because of a charge transfer from the acceptor to the σ^* orbital of the donor.

3.3 Geometries

Important geometrical parameters of 2MP and 2MP-water complexes are collected in Table 5. The DFT and MP2 are in general agreement with each other. The difference in computed bond lengths from two methods is in the range 0.0–0.005 Å and bond angle difference ranges from 0.0° to 0.4°. However, the difference of DFT and MP2 is greater for O···H and O···O distances and O–H···O angles as well as C4–O11–H12 angle. MP2 data will be given in parentheses in all subsequent discussions.

The length of phenolic O–H bond (O11–H12) in **1a** is equal to 0.970 (0.969) Å. This length changes to 0.982 (0.977) Å in **3** and 0.979 (0.976) Å in **4**, but in **5**, it remains constant at 0.970 (0.970) Å. This is because in **3** and **4**, H12 involves in an additional hydrogen bond compared to **1a**, therefore its length increases. This is in agreement with the observed red shift in O–H frequency (Table 4). In **5**, there is no additional hydrogen bond and the bond length remains unchanged.

Formation of O11···H19 hydrogen bond in **5** causes the bond length C4–O11 to change from 1.363 (1.367) Å in **1a** to 1.373 (1.376) Å. Similarly, because of O13···H19 hydrogen bond in **3**, the C5–O13 bond length which is equal to 1.377 (1.379) Å in **1a**, changes to 1.388 (1.388) Å In **4** and **5** these lengths are decreased. It is clear that upon hydrogen bond formation, the bonds with donor and acceptor atoms are both lengthened and in the case of hydrogen bond donor the increase is larger.

Similar effects are evident for water O–H bonds. The calculated O–H bond lengths in an isolated water molecule is 0.965 (0.961) Å. In **3**, the O18–H20 which does not take part in a hydrogen bond with 2MP molecule preserves this length; but O18–H19 which is a hydrogen bond donor lengthens to

Table 4 Calculated vibrational frequencies (cm^{-1}) for 2MP and three complexes

Frequency[a]	**1a**		**3**		**4**		**5**	
	B3LYP	MP2	B3LYP	MP2	B3LYP	MP2	B3LYP	MP2
Phenolic O–H	3, 688.2	3, 585.2	3, 443.7	3, 423.1	3, 521.3	3, 463.7	3, 685.5	3, 575.4
H_2O sym. O–H	–	–	–	–	3, 708.3	3, 626.5	–	–
H_2O asym. O–H	–	–	–	–	3, 813.6	3, 749.8	–	–
H_2O bonded O–H	–	–	3, 629.7	3, 576.7	–	–	3, 671.4	3, 605.9
H_2O free O–H	–	–	3, 784.3	3, 724.0	–	–	3, 793.8	3, 737.3

[a] B3LYP and MP2 frequencies are scaled by 0.978 and 0.937 factors, respectively [39,47]

Table 5 Optimized parameters (angstroms and degrees) for 2MP and three complexes

Parameter	**1a**		**3**		**4**		**5**	
	B3LYP	MP2	B3LYP	MP2	B3LYP	MP2	B3LYP	MP2
C1–C2	1.392	1.393	1.393	1.393	1.392	1.392	1.392	1.393
C2–C3	1.399	1.398	1.394	1.395	1.398	1.398	1.399	1.398
C3–C4	1.390	1.390	1.398	1.396	1.392	1.391	1.389	1.389
C4–C5	1.410	1.408	1.414	1.411	1.412	1.410	1.407	1.406
C5–C6	1.391	1.393	1.395	1.395	1.393	1.394	1.392	1.393
C6–C1	1.401	1.400	1.398	1.398	1.401	1.401	1.401	1.401
C4–O11	1.363	1.367	1.353	1.359	1.358	1.362	1.373	1.376
C5–O13	1.377	1.379	1.388	1.388	1.373	1.375	1.376	1.379
O13–C14	1.419	1.424	1.423	1.428	1.416	1.422	1.420	1.425
O11–H12	0.970	0.969	0.982	0.977	0.979	0.976	0.970	0.970
H12 $\cdots$ O13	2.076	2.061	2.386	2.346	2.172	2.130	2.069	2.050
O11$\cdots$O13	2.644	2.638	2.792	2.772	2.671	2.653	2.633	2.625
H12$\cdots$O18	–	–	1.822	1.872	1.955	1.994	–	–
O11$\cdots$O18	–	–	2.776	2.815	2.780	2.802	2.925	2.933
O13$\cdots$H19	–	–	1.918	1.943	–	–	–	–
O13$\cdots$O18	–	–	2.759	2.763	3.375	3.366	–	–
O11$\cdots$H19	–	–	–	–	–	–	2.008	2.016
O18$\cdots$H9	–	–	–	–	–	–	2.479	2.493
C3$\cdots$O18	–	–	–	–	–	–	3.356	3.366
O18–H19	–	–	0.973	0.968	0.967	0.964	0.970	0.967
O18–H20	–	–	0.966	0.963	0.967	0.964	0.965	0.962
C1–C2–C3	120.3	120.3	120.0	120.0	120.2	120.2	120.4	120.5
C2–C3–C4	119.9	119.8	121.3	121.0	120.4	120.1	119.3	119.1
C3–C4–C5	119.7	119.9	118.3	118.5	119.3	119.5	120.5	120.6
C4–C5–C6	120.3	120.5	120.3	120.5	120.3	120.4	120.0	120.1
C5–C6–C1	119.6	119.2	120.4	120.0	119.9	119.5	119.4	119.1
C6–C1–C2	120.2	120.4	119.6	119.8	120.0	120.2	120.4	120.5
C4–O11–H12	106.9	106.2	113.6	112.0	110.7	109.4	107.3	106.6
C5–C4–O11	120.0	120.1	124.2	123.8	121.1	120.7	119.3	119.3
C4–C5–O13	113.5	113.2	116.3	115.7	113.9	113.4	113.7	113.3
O11–H12$\cdots$O13	115.6	116.3	104.1	105.5	110.1	111.9	115.2	116.1
C5–O13$\cdots$H12	84.0	84.2	-	-	84.3	84.6	84.4	84.6
O11–H12$\cdots$O18	–	–	163.1	161.4	140.3	138.8	–	–
O13$\cdots$H19–O18	–	–	143.2	140.9	–	–	–	–
O11$\cdots$H19–O18	–	–	–	–	–	–	156.8	157.7
C3–H9$\cdots$O18	–	–	–	–	–	–	137.0	137.0
O13$\cdots$H12$\cdots$O18	–	–	–	–	109.6	109.4	–	–
H19–O18–H20	–	–	105.1	105.0	103.9	103.7	103.1	103.1

0.973 (0.968) Å. In **4**, water acts only as a hydrogen bond acceptor and its hydrogens are free. Therefore, there is a small and equal increase in water's bond lengths to 0.967 (0.964) Å. Finally in **5**, O18–H19 which forms the O11 $\cdots$ H19 − O18 hydrogen bond is 0.970 (0.967) Ålong, but O18–H20 remains constant at 0.965 (0.962) Å. These results are in accordance with frequency data.

The intramolecular hydrogen bond distance H12 $\cdots$ O13 in **1a** is 2.076 (2.061) Å. In **3** this hydrogen bond is lost and the distance reaches to 2.386 (2.346) Å. In **4**, this hydrogen bond is weakened to some extent and the interaction distance is 2.172 (2.130) Å. In structure **5**, there is a little decrease to 2.069 (2.050) Å. Two hydrogen bonds are present in each of three complexes and we can compare the strength of them

in each compound using the interaction distance. According to Table 5 in structure **3**, the H12···O18 hydrogen bond in which the water molecule acts as an acceptor is stronger than the O13···H19 hydrogen bond. The H12···O18 intermolecular hydrogen bond in **4** is much stronger than the H12···O13 intramolecular bond. Also in **5**, the intermolecular interaction (O11···H19) is slightly stronger than intramolecular (H12···O13) hydrogen bond.

The hydrogen bond length O11···O13 in **1a** is 2.644 (2.638) Å. As the H12···O13 distance in **4** increases, this length also increases to 2.671 (2.653) Å. In **5** this length reduces to 2.633 (2.625) Å. Formation of a 7-membered ring in **3** causes these atoms to become distant and their distance reaches to 2.792 (2.772) Å. The O11···O18 distance in **3**, **4** and **5** is equal to 2.776 (2.815), 2.780 (2.802) and 2.925 (2.933) Å, respectively, which shows a gradual decrease in the intermolecular hydrogen bond strength in line with an increase in the corresponding O···H distance. It seems that it is not possible to make use of O···O distance for the comparison of hydrogen bond strengths in any of three structures. This distance behaves in the opposite direction of the O···H distance; it increases as the O···H distance decreases.

Hydrogen bond angles (O–H···O) for intermolecular hydrogen bonds are close to 180°[163.1°(161.4°) for O11–H12···O13 and 143.2°(140.9°) for O18–H19···O13 in **3**; 156.8°(157.7°) for O18–H19···O11 in **5**]. This angle is about 120° for intramolecular hydrogen bonds (Table 5). In 2MP and **4** and **5** complexes, the atoms involving in hydrogen bonds are almost coplanar, but for **3** there is a little deviation of 18.0°(19.1°) from planarity. The bifurcated hydrogen bond in **4** is not symmetric, as it is clear from the difference in H12···O13 and H12···O18 distances. The sum of three valence bond angles which are formed by H12 and three oxygen atoms (O11, O13 and O18) is equal to 360°; that is, all four atoms lie in same plane.

The H–O–H angle in a free water molecule is 103.7° (103.8°). This angle remains more or less constant in **4** and slightly decreases in **5**. In **3**, because of geometrical requirements, this angle expands to 105.1°(105.0°).

The C4–O11–H12, C5–C4–O11 and C4–C5–O13 in **1a** are equal to 106.9°(106.2°), 120.0°(120.1°) and 113.5° (113.2°), respectively. All these angles increase in **3**, because of the geometric requirements of a 7-membered ring; but remain constant in **4** and **5**.

An additional hydrogen bond of the type C–H···O can be formed between H9 and O18 in **5**. The distance of H9···O18 interaction and the C3–H9···O18 are in the observed range for a series of C–H···O hydrogen bonds [29].

According to Table 5, the bond lengths of the benzene ring in **1a** represent that C1–C2, C3–C4 and C5–C6 are double bonds. This situation continues in **4** and **5**. But in **3**, C4–C5, C3–C4 and C5–C6 bonds lengthen and C1–C6 and C2–C3 bonds shorten to allow a 7-ring to form. There is no special change in terms of electron distribution that represents resonance structures.

3.4 NBO analysis

3.4.1 Natural population analysis

The charges obtained from NPA for all molecules are listed in Table 6. The charges on benzene ring's atoms have not changed very much upon complexation. In an isolated water molecule, the calculated NPA charge for oxygen atom is −0.944 (−0.970) au and for each of hydrogen atoms is 0.472 (0.485) au After complex formation in **3**, O18 atom (of water) becomes more negative and the positive charge on H19 and H20 increases. This increase is not equal for two hydrogen atoms. Because H19 involves in O13···H19 hydrogen bond, it experiences a larger increase. Similar changes are observed for **4** and **5**. But for complex **4**, the amount of change is very small and the charge on two hydrogen atoms increases by the same amount.

The charge on O13 atom of **1a** is −0.552 (−0.635) au which becomes more negative as it forms an intermolecular hydrogen bond in **3**. In **4**, the intramolecular O13···H12 hydrogen bond weakens and O13 becomes less negative. The

Table 6 Natural population analysis (NPA) charges for model systems

Atom	**1a**		**3**		**4**		**5**	
	B3LYP	MP2	B3LYP	MP2	B3LYP	MP2	B3LYP	MP2
C1	−0.254	−0.249	−0.259	−0.255	−0.258	−0.251	−0.249	−0.241
C2	−0.247	−0.234	−0.244	−0.228	−0.251	−0.237	−0.245	−0.234
C3	−0.286	−0.281	−0.282	−0.281	−0.289	−0.285	−0.285	−0.279
C4	0.295	0.341	0.299	0.349	0.297	0.344	0.286	0.327
C5	0.247	0.283	0.237	0.268	0.250	0.287	0.250	0.288
C6	−0.311	−0.302	−0.305	−0.293	−0.314	−0.305	−0.311	−0.304
H7	0.239	0.235	0.239	0.235	0.237	0.233	0.241	0.237
H8	0.240	0.236	0.240	0.236	0.237	0.234	0.243	0.238
H9	0.250	0.248	0.250	0.248	0.245	0.243	0.264	0.265
H10	0.241	0.238	0.239	0.236	0.239	0.236	0.242	0.239
O11	−0.696	−0.766	−0.715	−0.788	−0.725	−0.797	−0.724	−0.793
H12	0.506	0.524	0.514	0.544	0.517	0.545	0.516	0.534
O13	−0.552	−0.635	−0.568	−0.650	−0.538	−0.622	−0.553	−0.636
C14	−0.322	−0.242	−0.324	−0.244	−0.322	−0.242	−0.322	−0.242
H15	0.209	0.194	0.217	0.202	0.205	0.190	0.210	0.195
H16	0.232	0.216	0.231	0.216	0.233	0.219	0.232	0.217
H17	0.209	0.194	0.207	0.191	0.205	0.190	0.211	0.196
O18	–	–	−0.963	−1.002	−0.947	−0.980	−0.969	−1.000
H19	–	–	0.502	0.520	0.490	0.499	0.494	0.514
H20	–	–	0.486	0.495	0.490	0.499	0.469	0.481

charge on O13 does not change in complex **5**. The positive charge on H12 atom in **3**, **4**, and **5** is larger than **1a**. MP2 method generally results more positive charges than DFT.

3.4.2 Energy delocalization and charge distribution

In the NBO method, all possible interactions between "filled" (electron-donor) Lewis-type NBOs and "empty" (electron-acceptor) non-Lewis NBOs are examined and the energetic importance of each interaction is estimated by second-order perturbation theory. For each donor NBO (i) and acceptor NBO (j), the stabilization energy associated with delocalization $i \rightarrow j$ is estimated by

$$E^{(2)} = q_i \frac{F(i,j)^2}{\varepsilon_j - \varepsilon_i}$$

where q_i is donor orbital occupancy, ε_j and ε_i are diagonal elements (orbital energies), and $F(i, j)$ is the off-diagonal NBO Fock matrix element. In hydrogen-bonded systems, the delocalization from hydrogen bond acceptor's lone pair to σ^* orbital of the donor group usually occurs. (that is, $n_Y \rightarrow \sigma^*$(X–H) in a X–H$\cdots$Y hydrogen bond) [43].

The NBO analysis of the wavefunctions provides information about charge distribution over the molecules. The amount of $n_Y \rightarrow \sigma^*$(X–H) charge transfer can be estimated by [46]:

$$q_{n\rightarrow\sigma^*} \approx 2\left\{F\left(n,\sigma^*\right)/\left(\varepsilon_{\sigma^*} - \varepsilon_n\right)\right\}^2$$

Table 7 summarizes the most important donor-acceptor interactions in 2MP and three complexes. The delocalization energy for n_1(O13) $\rightarrow$ σ^*(O11–H12) interaction in **1a** is 3.36 (4.03) kcal/mol. This energy reduces to 2.86 (3.76) kcal/mol in **4** in accord with other evidences for the reduction of intramolecular hydrogen bond strength. In **5**, a little increase to 3.50 (4.28) kcal/mol is observed. In structure **3**, there are three important donor-acceptor interactions. The strongest interaction is for n_2(O18) $\rightarrow$ σ^*(O11–H12), which has $E^{(2)}$ value of 18.82 (17.92) kcal/mol. The second important interaction is n_1(O13) $\rightarrow$ σ^*(O18–H19) in which a lone pair with $\sim$ 63% p- character interacts with σ^* orbital of O18–H19. It is clear that the O18$\cdots$H12 hydrogen bond is stronger than H19$\cdots$O13 hydrogen bond. The weakest interaction is n_2(O13) $\rightarrow$ σ^*(O18–H19), in which a lone pair of oxygen with $\sim$98% p-character is involved. Finally, the corresponding interaction energies for H12$\cdots$O13 and O11$\cdots$H19 hydrogen bonds in **5** are 3.50 (4.28) and 7.17 (7.98) kcal/mol, respectively. There is also a weak interaction n_2(O18) $\rightarrow$ σ^*(C3–H9) corresponding to C3–H9$\cdots$O18 hydrogen bond. The energy associated with this interaction is 2.13 (2.16) kcal/mol. There is correlation between the interaction energy and amount of charge transferred to σ^* orbitals: the lower the delocalization energy, the lower is charge transferred.

3.5 Atoms in Molecules Analysis

The total topology of 2MP and all three complexes is consistent with the Poincaré-Hopf relationship. The critical point properties for various covalent and hydrogen bonds from DFT and MP2 methods are given in Tables 8 and 9, respectively. As it is clear from these tables, all BCPs and RCPs are present at expected places. The charge density (ρ) and the Laplacian of charge density ($\nabla^2\rho$) at hydrogen BCPs are all in the proposed range of 0.002–0.034 au and 0.024–0.139 au, respectively [29].

The charge density at BCP for hydrogen bonds is an order of magnitude smaller than for the corresponding covalent bonds. The Laplacian of charge density, $\nabla^2\rho$ is positive for H-bonds, in contrast to covalent bonds.

The superposition of charge density contour maps together with molecular graphs and interatomic surfaces are depicted in Fig. 2 for 2MP and three complexes. The BCPs and RCPs are located in the right places in a bond path that connects atoms involved in a hydrogen bond. The interaction between H9 and O18 atoms in **5** is a rather strong H-bond.

Table 7 Natural bond orbital (NBO) analysis for model systems

Molecule	Interaction	$E^{(2)}$, kcal mol^{-1}		q, au		% p (n_O)	
		B3LYP	MP2	B3LYP	MP2	B3LYP	MP2
1a	n_1(O13) $\rightarrow$ σ^*(O11–H12)	3.36	4.03	0.005281	0.004075	61.65	62.41
3	n_1(O13) $\rightarrow$ σ^*(O18–H19)	7.54	7.22	0.011686	0.007281	62.81	63.96
	n_2(O13) $\rightarrow$ σ^*(O18–H19)	1.96	2.37	0.003798	0.002835	98.67	98.40
	n_2(O18) $\rightarrow$ σ^*(O11–H12)	18.82	17.92	0.034649	0.020899	90.36	88.75
4	n_1(O13) $\rightarrow$ σ^*(O11–H12)	2.86	3.76	0.004421	0.003787	61.55	62.26
	n_2(O18) $\rightarrow$ σ^*(O11–H12)	12.39	11.94	0.022494	0.013562	87.17	86.42
5	n_1(O13) $\rightarrow$ σ^*(O11–H12)	3.50	4.28	0.005385	0.004308	61.68	62.42
	n_1(O11) $\rightarrow$ σ^*(O18–H19)	7.17	7.98	0.010194	0.007690	56.24	57.63
	n_2(O18) $\rightarrow$ σ^*(C3–H9)	2.13	2.16	0.004357	0.002687	97.64	97.16

Table 8 Critical point properties calculated at B3LYP/6-31G(d,p) level of theory

	Interaction	ρ	$\nabla^2\rho$	ε	λ_1	λ_2	λ_3	rBR
1a	H12···O13	2.09×10^{-2}	8.36×10^{-2}	4.22×10^{-1}	-2.36×10^{-2}	-1.66×10^{-2}	1.24×10^{-1}	0.52
	O11–H12	3.61×10^{-1}	−2.08	2.26×10^{-2}	−1.842	−1.802	1.563	–
3	O11–H12	3.42×10^{-1}	−1.99	1.91×10^{-2}	−1.792	−1.758	1.563	–
	O13···H19	2.81×10^{-2}	8.40×10^{-2}	9.34×10^{-2}	-3.82×10^{-2}	-3.50×10^{-2}	1.57×10^{-1}	1.72
	H12···O18	3.55×10^{-2}	9.72×10^{-2}	2.48×10^{-2}	-5.23×10^{-2}	-5.11×10^{-2}	2.00×10^{-1}	1.75
	O18–H19	3.53×10^{-1}	−2.05	2.46×10^{-2}	−1.827	−1.783	1.557	–
	O18–H20	3.63×10^{-1}	−2.05	2.36×10^{-2}	−1.804	−1.763	1.521	–
4	O11–H12	3.47×10^{-1}	−2.04	1.98×10^{-2}	−1.817	−1.782	1.562	–
	H12···O13	1.75×10^{-2}	8.08×10^{-2}	3.79	-1.81×10^{-2}	-3.77×10^{-3}	1.03×10^{-1}	0.13
	H12···O18	2.72×10^{-2}	7.44×10^{-2}	5.03×10^{-2}	-3.67×10^{-2}	-3.50×10^{-2}	1.46×10^{-1}	2.80
	O18–H19	3.63×10^{-1}	−2.05	2.69×10^{-2}	−1.814	−1.766	1.527	–
	O18–H20	3.63×10^{-1}	−2.05	2.69×10^{-2}	−1.814	−1.767	1.527	–
5	O11–H12	3.59×10^{-1}	−2.09	2.36×10^{-2}	−1.851	−1.809	1.571	–
	H12···O13	2.12×10^{-2}	8.40×10^{-2}	3.79×10^{-1}	-2.40×10^{-2}	-1.74×10^{-2}	1.25×10^{-1}	0.54
	O11···H19	2.19×10^{-2}	6.40×10^{-2}	4.65×10^{-2}	-2.79×10^{-2}	-2.66×10^{-2}	1.19×10^{-1}	1.85
	H9···O18	1.07×10^{-2}	3.20×10^{-2}	1.42×10^{-1}	-1.11×10^{-2}	-9.69×10^{-3}	5.27×10^{-2}	1.52
	O18–H19	3.57×10^{-1}	−2.06	2.73×10^{-2}	−1.828	−1.780	1.551	–
	O18–H20	3.65×10^{-1}	−2.02	2.74×10^{-2}	−1.784	−1.737	1.499	–

Table 9 Critical point properties calculated at MP2/6-31G(d,p) level of theory

	Interaction	ρ	$\nabla^2\rho$	ε	λ_1	λ_2	λ_3	rBR
1a	H12···O13	2.17×10^{-2}	8.88×10^{-2}	4.58×10^{-1}	-2.41×10^{-2}	-1.66×10^{-2}	1.29×10^{-1}	0.49
	O11–H12	3.59×10^{-1}	−2.07	2.47×10^{-2}	−1.830	−1.786	1.543	–
3	O11–H12	3.45×10^{-1}	−2.04	2.13×10^{-2}	−1.819	−1.781	1.554	–
	O13···H19	3.12×10^{-2}	8.96×10^{-2}	2.21×10^{-2}	-4.33×10^{-2}	-4.23×10^{-2}	1.75×10^{-1}	1.66
	H12···O18	2.65×10^{-2}	8.32×10^{-2}	1.12×10^{-1}	-3.50×10^{-2}	-3.14×10^{-2}	1.50×10^{-1}	1.68
	O18–H19	3.65×10^{-1}	−2.09	2.62×10^{-2}	−1.843	−1.796	1.551	–
	O18–H20	3.64×10^{-1}	−2.06	2.56×10^{-2}	−1.812	−1.767	1.519	–
4	O11–H12	3.47×10^{-1}	−2.07	2.21×10^{-2}	−1.828	−1.789	1.549	
	H12···O13	1.91×10^{-2}	8.64×10^{-2}	1.759	-2.00×10^{-2}	-7.26×10^{-3}	1.14×10^{-1}	0.23
	H12···O18	2.49×10^{-2}	7.20×10^{-2}	4.98×10^{-2}	-3.22×10^{-2}	-3.07×10^{-2}	1.35×10^{-1}	2.85
	O18–H19	3.64×10^{-1}	−2.07	2.84×10^{-2}	−1.821	−1.770	1.523	–
	O18–H20	3.64×10^{-1}	−2.07	2.84×10^{-2}	−1.821	−1.770	1.523	–
5	O11–H12	3.57×10^{-1}	−2.08	2.54×10^{-2}	−1.836	−1.790	1.549	–
	H12···O13	2.22×10^{-2}	8.96×10^{-2}	3.96×10^{-1}	-2.48×10^{-2}	-1.78×10^{-2}	1.32×10^{-1}	0.53
	O11···H19	2.11×10^{-2}	6.52×10^{-2}	5.03×10^{-2}	-2.63×10^{-2}	-2.50×10^{-2}	1.17×10^{-1}	1.83
	H9···O18	1.04×10^{-2}	3.30×10^{-2}	1.45×10^{-1}	-1.07×10^{-2}	-9.30×10^{-3}	5.29×10^{-2}	1.49
	O18–H19	3.59×10^{-1}	−2.09	2.84×10^{-2}	−1.843	−1.793	1.547	–
	O18–H20	3.67×10^{-1}	−2.04	2.86×10^{-2}	−1.797	−1.747	1.503	–

There are criteria for the strength of a hydrogen bond based on the AIM theory. The first criterion is related to ellipticity. Larger ellipticity corresponds with a weaker interaction. As it is obvious from the data, the ellipticity values for the intramolecular hydrogen bond in 2MP and **5** are very similar, indicating that the intramolecular hydrogen bond is conserved in complex **5**. In contrast, this value for H12···O13 interaction in **4** is very larger than 2MP, which is the result of a weak interaction. The second criterion concerns the distance of a BCP from the closest RCP to it (rBR). This

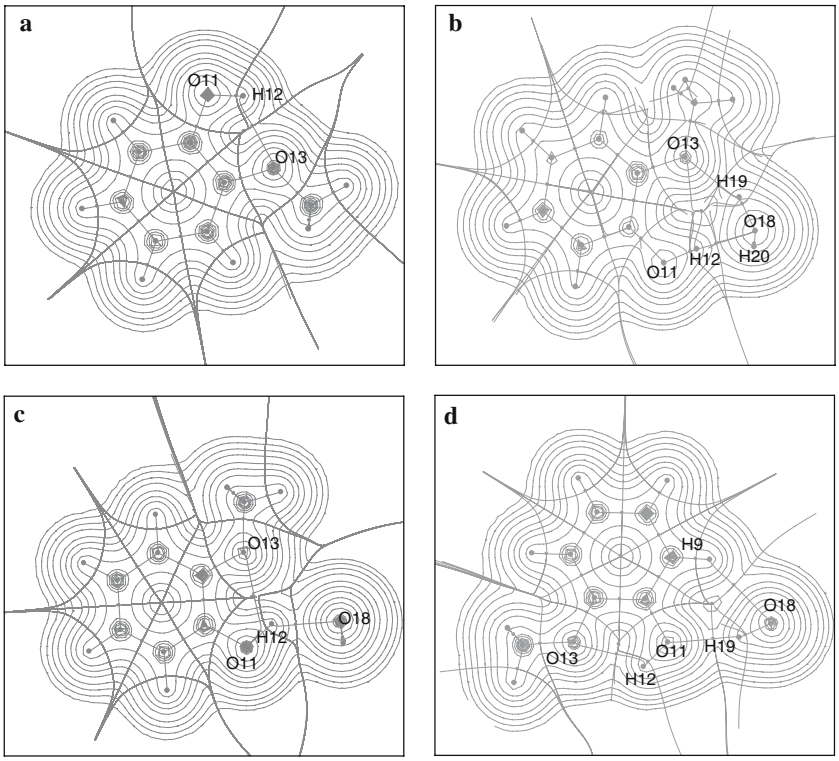

Fig. 2 bond paths and interatomic surfaces (in *bold*) superimposed on the electron density contour lines (*thin*) for 2MP (**a**) and three complexes (**b–d**). Bond critical points and ring critical points are denoted by *squares*

distance is calculated for hydrogen bond BCPs and shows that the intermolecular hydrogen bonds are stronger than the intramolecular hydrogen bonds.

It is possible to compare the strength of two bifurcated hydrogen bonds in complex **4**. In agreement to bond length data, the hydrogen bond between H12 and O18 (intermolecular) is much more stable than the H12$\cdots$O13 (intramolecular) interaction. This is due to a larger ellipticity and closer distance to RCP for the latter case. The ellipticity for H12$\cdots$O13 interaction is about 2 orders of magnitude greater than for H12$\cdots$O18 bond. Also, the BCP to RCP distance for H12$\cdots$O13 is very small. The parameters for two O–H BCPs of water in structure **4** are virtually equal, showing the equivalence of these two bonds in that complex.

The AIM data obtained from DFT and MP2 are very similar to each other. The only significant difference is in rBR and ellipticity values for H12$\cdots$O13 interaction in **4**. MP2 calculations suggest a more stable intramolecular hydrogen bond.

4 Conclusion

DFT and MP2 calculations confirm the proposed structure for three hydrogen-bonded clusters of 2-methoxyphenol and water. The energies, frequencies and geometrical data obtained from MP2 method are in better agreement with experimental data. MP2 also shows a more stable interaction for complex **4**. The most stable complex based on energetic, geometrical and topological data is **3**. From energy data including ZPE corrections, structure **4** is more stable than **5**. It is motivating to find the conditions to make this special bifurcated structure more stable.

References

1. de Heer MI, Mulder P, Korth H-G, Ingold KU, Lusztyk J (2000) J Am Chem Soc 122:2355–2360
2. Avila DV, Ingold KU, Lusztyk J (1995) J Am Chem Soc 117:2929–2930
3. de Heer MI, Korth H-G, Mulder P (1999) J Org Chem 64:6969–6975
4. Wright JS, Carpenter DJ, McKay DJ, Ingold KU (1997) J Am Chem Soc 119:4245–4252
5. Palusiak M, Grabowski SJ (2002) J Mol Struct 642:97–104
6. Spencer JN, Robertson KS, Quick EE (1974) J Phys Chem 78:2236–2240
7. Spencer JN, Heckman RA, Harner RS, Shoop SL, Robertson KS (1973) J Phys Chem 77:3103–3106
8. Fain AV, Berezovsky IN, Chekhov VO, Ukrainskii DL, Esipova NG (2001) Biophysics 46:921–928
9. Meyer M, Brandl M, Sühnel J (2001) J Phys Chem A 105:8223–8225
10. Newton MD, Jeffrey GA, Takagi S (1979) J Am Chem Soc 101:1997–2002
11. Kerns RC, Allen LC (1978) J Am Chem Soc 100:6587–6594
12. Kollman PA, Allen LC (1970) J Am Chem Soc 92:753–759
13. Rozas I, Alkorta I, Elguero J (1998) J Phys Chem A 102:9925–9932
14. Kovács A, Hargittai I (1998) J Phys Chem A 102:3415–3419

15. Bureiko SF, Golubev NS, Pihlaja K (1999) J Mol Struct 480–481:297–301
16. Zheng J, Kwak K, Chen X, Asbury JB, Fayer MD (2006) J Am Chem Soc 128:2977–2987
17. Wu R, Brutschy B (2004) Chem Phys Lett 390:272–278
18. Mitsuzuka A, Fujii A, Ebata T, Mikami N (1998) J Phys Chem A 102:9779–9784
19. Wu R, Vaupel S, Nachtigall P, Brutschy B (2004) J Phys Chem A 108:3338–3343
20. Nibu Y, Marui R, Shimada H (2006) J Phys Chem A 110:9627–9632
21. Matsumoto Y, Ebata T, Mikami N (2000) J Mol Struct 552:257–271
22. Yokoyama H, Watanabe H, Omi T, Ishiuchi S-i, Fujii M (2001) J Phys Chem A 105:9366–9374
23. Venkatesan V, Fujii A, Ebata T, Mikami N (2005) J Phys Chem A 109:915–921
24. Li Y, Liu X-H, Wang X-Y, Lou N-Q (1999) J Phys Chem A 103:2572–2579
25. Li S, Weber KH, Tao F-M, Gu R (2006) Chem Phys 323:397–406
26. Zhang B, Cai Y, Mu X, Lou N, Wang X (2002) Chem Phys 276:277–292
27. Jalili S, Akhavan M (2004) J Theor Comput Chem 3:527–542
28. Buemi G, Zuccarello F (2002) J Mol Struct THEOCHEM 581:71–85
29. Koch U, Popelier PLA (1995) J Phys Chem 99:9747–9754
30. Bader RFW (1990) Atoms in molecules—a quantum theory. Oxford University Press, New York
31. Matta CF, Boyd RJ (2007) The quantum theory of atoms in molecules. In: From solid state to DNA and drug design, Wiley-VCH Verlag GmbH & Co, KGaA, Weinheim
32. Hocquet A (2001) Phys Chem Chem Phys 3:3192–3199
33. Popelier PLA (1998) J Phys Chem A 102:1873–1878
34. Louit G, Hocquet A, Ghomi M, Meyer M, Sühnel J (2002) Phys Chem Comm 5:94–98
35. Jalili S, Soleimani M (2006) J Theo Comput Chem 5:633–645
36. Frisch MJ, Trucks GW, Schlegel HB, Scuseria GE, Robb MA, Cheeseman JR, Montgomery JA Jr, Vreven T, Kudin KN, Burant JC, Millam JM, Iyengar SS, Tomasi J, Barone V, Mennucci B, Cossi M, Scalmani G, Rega N, Petersson GA, Nakatsuji H, Hada M, Ehara M, Toyota K, Fukuda R, Hasegawa J, Ishida M, Nakajima T, Honda Y, Kitao O, Nakai H, Klene M, Li X, Knox JE, Hratchian HP, Cross JB, Adamo C, Jaramillo J, Gomperts R, Stratmann RE, Yazyev O, Austin AJ, Cammi R, Pomelli C, Ochterski JW, Ayala PY, Morokuma K, Voth GA, Salvador P, Dannenberg JJ, Zakrzewski VG, Dapprich S, Daniels AD, Strain MC, Farkas O, Malick DK, Rabuck AD, Raghavachari K, Foresman JB, Ortiz JV, Cui Q, Baboul AG, Clifford S, Cioslowski J, Stefanov BB, Liu G, Liashenko A, Piskorz P, Komaromi I, Martin RL, Fox DJ, Keith T, Al-Laham MA, Peng CY, Nanayakkara A, Challacombe M, Gill PMW, Johnson B, Chen W, Wong MW, Gonzalez C, Pople JA (2003) Gaussian 03 Gaussian, Inc., Pittsburgh, PA
37. Biegler-König F, Schönbohm J, Bayles D (2001) J Comput Chem 22:545–559
38. Jalili S, Akhavan M (2006) J Mol Struct THEOCHEM 765:105–114
39. Scott AP, Radom L (1996) J Phys Chem 100:16502–16513
40. Del Bene JE (1995) J Phys Chem 99:10705–10707
41. Jensen F (1996) Chem Phys Lett 261:633–636
42. Carpenter JE, Weinhold F (1988) J Mol Struct THEOCHEM 169:41–62
43. Reed AE, Curtiss LA, Weinhold F (1988) Chem Rev 88:899–926
44. Reed AE, Weinstock RB, Weinhold F (1985) J Chem Phys 83:735–746
45. Glendening ED, Reed AE, Carpenter JE, Weinhold F (1992) NBO, Version 3.1, Gaussian Inc., Pittsburgh, PA
46. Parra RD, Bulusu S, Zeng XC (2005) J Chem Phys 122:184325
47. Szczepanski J, Dibben MJ, Pearson W, Eyler JR, Vala M (2001) J Phys Chem A 105:9388–9395